

Monitoring Urban Landscape of Taiwan Using PALSAR Data

Pu-Huai Chen⁽¹⁾, Ian Dowman⁽²⁾

⁽¹⁾ Dept. of Information Management, Kainan University, Luchu, Taoyuan 33857, Taiwan ROC, E-mail: phchen@mail.knu.edu.tw

⁽²⁾ Dept. of Geomatic Eng., University College London, Gower St., London WC1E 6BT, U.K., E-mail: idowman@ge.ucl.ac.uk

Abstract

ALOS PALSAR intensity images with dual polarization (HH/HV) taken at nadir angle of 41.5 degrees are studied to evaluate the limitations and possibilities of urban mapping using L-band SAR data in Taiwan. At this stage, it is suggested that integration of PALSAR data with dual polarization is potentially useful for mapping the pattern of building blocks of urban Taipei with a wide scope. In terms of town planning and urban renewal projects, PALSAR data could be useful in monitoring redevelopment of open space as well as in understanding SAR signatures of different types of land-cover. However, it is also found that great care has to be taken in interpretation and segmentation of SAR images with single polarization (HH or HV).

Keywords: Urban Landscape, PALSAR, Image Analysis, Polarization

1. INTRODUCTION

Traditional applications of SAR data are being focused at rural environment observation, such as agricultural activity survey, natural phenomena investigation and disaster monitoring, but urban analysis and mapping applications have attracted more attention in the past decade [1][2][3][4]. Work has been carried out on urban mapping using SAR images, but there is no guarantee of successful application under all circumstances [5][6][7]. In addition, there is no universal solution for understanding SAR images of urban areas at this stage [8][9].

SAR images of urban areas taken from different locations may show different spatial and radiometric characteristics. For instance, strategies of town planning and construction regulations at various socio-economic stages can strongly influence the urban development of a city [10][11], giving a heterogeneous pattern in SAR intensity image. As far as urban mapping is concerned, the factors leading to ambiguities in SAR image classification and texture analysis have to be identified in the first place. Thus, this paper is aimed at finding some of the key factors that affects visual and automatic understanding for SAR imagery. The recent development of space-borne SAR systems provides new opportunities for understanding urban landscape in various aspects. For instance it is proposed that the Advanced Land Observation Satellite (ALOS) Phased Array L-type Synthetic Aperture Radar (PALSAR) images with dual polarization (HH+HV), as

described in the following sections, can be used for mapping the building block pattern in urban environments. Also, some of the factors that characterize urban landscape, such as open space (sport fields, playgrounds and parks) giving relatively low intensity levels, can be detected in PALSAR images with dual polarization using relatively simple algorithms.

In Section 2, the algorithms proposed are aimed at solving the problems arising at the primitive stage of SAR image understanding, including validation on the intensity levels of different types of land-cover or water. The proposed algorithm for mapping the building block pattern is tested using ellipsoid corrected geo-referenced PALSAR data taken in northern Taiwan, as described in Section 3. Brief discussion and conclusions are given in Section 4 and 5, respectively.

2. THEORY

In the context of urban environments, extended targets in a single SAR image can be perceived and classified as dark and bright features by a human operator. In general, the bright features indicate built-up areas and significant facilities, such as bridges or railways. The dark features may be referred to as pavement of roads, runways, parks or water. It is proposed in this paper that the dark features can be employed as a comparative basis in radiometry for other brighter targets in the context of urban environments. Let int_d be the averaged intensity level $(DN)_d$ of n pixels sampled from dark features and int_b be the averaged intensity level $(DN)_b$ of n pixels sampled from bright features, then, the ratio of intensity levels between the bright and the dark one gives σ_d (in dB) as

$$\sigma_d = 10 \log_{10} \frac{\text{int}_b}{\text{int}_d} \quad (1)$$
$$\text{int}_d = \frac{1}{n} \sum_{i=1}^n [(DN)_d]_i ; \quad \text{int}_b = \frac{1}{n} \sum_{i=1}^n [(DN)_b]_i$$

Co-polarized (HH or VV) and cross-polarized (HV or VH) SAR images may demonstrate distinct characteristics of extended targets in urban environments. For instance, cross-polarized images are expected to be less sensitive to Bragg scattering since roof structure with a periodic pattern tends to reflect the major part of co-polarized signal power in comparison with the co-polarized counterpart. Furthermore, the Bragg condition can happen only if the

sensor-target orientation is perfectly aligned with the SAR range direction. Then, layover effect and Bragg scattering can be discriminated using SAR data with dual polarization since the former can still backscatter signal power at certain level when the sensor-target orientation is not aligned with the SAR range direction.

A practical tool for visualizing different kinds of building block pattern in SAR images with dual polarization is proposed as followed. The intensity levels of SAR images are designated as \mathbf{int}_{HH} and \mathbf{int}_{HV} for HH and HV-polarized image, respectively. Both images are first reduced to 8-bit dynamic range and then enhanced to achieve the same (or similar) image statistics by using histogram normalization. Secondly, logical operations are required for obtaining pixels of the maximal intensity and the minimal one, giving as \mathbf{int}_{\max} and \mathbf{int}_{\min} , respectively. Also, a difference image $\mathbf{int}_{\text{diff}}$ can be derived as followed.

$$\begin{aligned} \mathbf{int}_{\max} &= \max(\mathbf{int}_{HH}, \mathbf{int}_{HV}) \Rightarrow \text{Red} \\ \mathbf{int}_{\min} &= \min(\mathbf{int}_{HH}, \mathbf{int}_{HV}) \Rightarrow \text{Green} \\ \mathbf{int}_{\text{diff}} &= 0.5 \times \text{abs}(\mathbf{int}_{HH} - \mathbf{int}_{HV} + 1) + 127 \Rightarrow \text{Blue} \end{aligned} \quad (2)$$

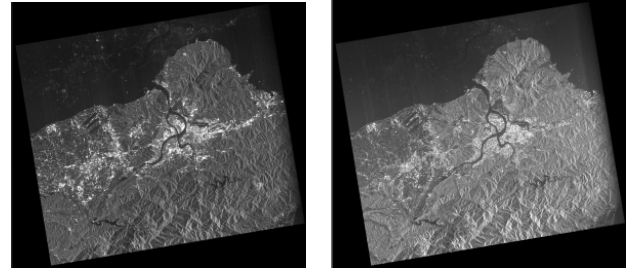
The maximal intensity image, $\max(\mathbf{int}_{HH}, \mathbf{int}_{HV})$, is designated as red colour, the minimal intensity image, $\min(\mathbf{int}_{HH}, \mathbf{int}_{HV})$, as green and the difference image as blue, then a colour-coded image can be used to produce a building block pattern map in urban areas.

3. TEST RESULTS

3.1 Test Data

Urbanization in new industrialized economies, such as Taiwan, faces difficulties in finding a balance between the needs of housing supply and good quality of urban environments. The urban landscape as seen in Taipei City is extremely crowded, and improvement of transportation, as well as urban renewal, are desired. City block patterns may affect future transportation improvement and urban renewal projects, and SAR imagery might provide alternative ways to map city block patterns. Taipei City is suitable as the test area in the study since it can be treated as a model for other urban areas in Taiwan, where building block patterns are more or less the same. Full scenes of ALOS PALSAR image (Polarization: HH and HV) taken on 17th Oct 2006 centred on Taipei, Taiwan, are employed for verification of intensity levels of dark and bright features, as shown in Fig.1. Some examples of the statistics for the averaged intensity levels of the image tiles observed in the HH-polarized PALSAR image of various land-cover types, such as urban area, vegetation, pavement, river and sea, are demonstrated as in Table 1. The statistics of image tiles are derived based on 8-bit data reduced from the original 16-bit image. The size of each sampled image tile varies from 9 by 9 pixels at urban area

to 100 by 100 pixels at sea. The ratio of intensity levels shows that urban areas are distinct in radiometry from other types of land-cover and water.



© JAXA

Figure 1 Full scenes of ALOS PALSAR geo-referenced image with polarization HH and HV taken on 17th Oct 2006 in northern Taiwan at angle of incidence $\theta = 41.5$ degrees; near-range is at the left. Resolution: 12.5m; image size: 6200 lines by 6896 pixels.

Table 1 The statistics of the averaged intensity levels of the measured and sampled 8-bit image tiles regarding to different land-cover types (unit: intensity level 0~255)

Intensity	Sea	River	Pavement	Vegetation	Urban
Average	6.6	10.9	12.0	13.5	39.9
Std. Dev.	1.4	2.3	2.4	2.9	18.9
Maximal	7.8	14.1	12.9	16.2	133.7
Minimal	4.8	8.0	11.4	11.1	17.7
Samples	10000	441	81~441	36~729	81~961
Ratio (dB)	-1.4~0.7	0.8~3.3	2.4~2.9	2.3~3.1	4.3~13

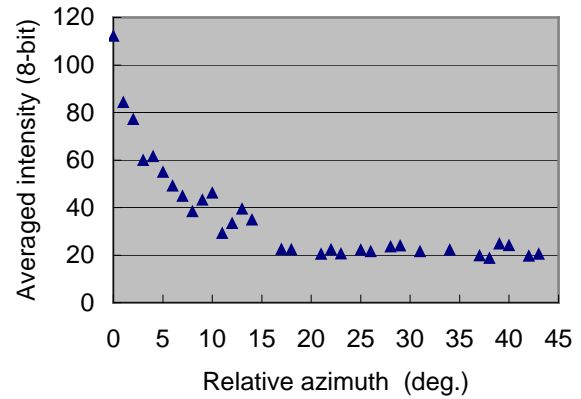


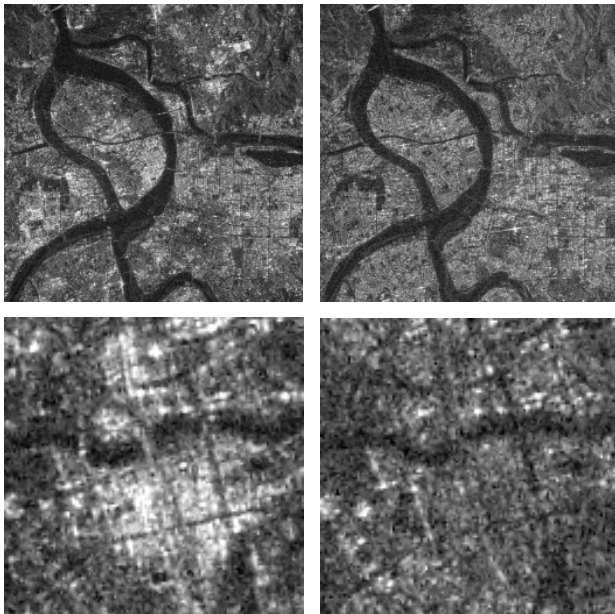
Figure 2 The averaged intensity of building blocks vs. relative azimuth regarding to the sensor-target orientation derived from urban areas in the full scenes of ALOS PALSAR geo-referenced imagery with HH and HV polarization taken on 17th Oct 2006 in northern Taiwan.

In order to understand the trend of relative intensity levels of built-up areas due to the sensor-target orientation, intensity statistics of image tiles regarding to the relative azimuth of building blocks in urban areas are measured and

summarized as in Fig. 2. Each image tile may contain different number of pixels ranging from 9 by 9 pixels to 31 by 31 pixels, depending on the availability of building blocks.

3.2 Building-Block Pattern Map Derived from SAR Intensity Images with Dual Polarization

Sub-scenes extracted from the ALOS PALSAR images (Polarization: HH & HV), as shown in Fig. 3, are employed for mapping the building block pattern of Taipei. There are some significant bright areas observed in the HH-polarized image. Fig. 3 also gives an example showing that Bragg scattering or strong dihedral reflection occurs when the block azimuth is in parallel with range direction. These effects are quite significant on intensity levels of HH-polarized images, which can mislead the results of SAR image interpretation and segmentation. Considering surface (roof) structure and building block azimuth, it is proposed that integration of HH- and HV-polarized images could be useful in mapping block pattern.



© JAXA

Figure 3. Sub-scenes extracted from those in Fig. 1 of polarization: HH (left) and HV (right), illuminated from the left (resolution: 12.5m; size: 1024 by 1024 pixels). One of the bright areas in the HH-polarized image (bottom-left size: 128 by 128 pixels) is shown with the HV-polarized counterpart (bottom-right).

The method proposed in Section 2 is employed to produce a colour-coded image map of building block patterns, as shown in Fig. 4a. The magenta-coloured areas denote strong backscattering by layover, dihedral reflection and Bragg condition due to the block azimuth in parallel with the SAR range direction. The relative azimuth in these brightest areas is measured as within 2 degrees with respect to the range direction. The areas coloured yellow show

less bright intensity levels, and the relative azimuth of the block pattern is falling into the range of 3-15 deg. with respect to either side of the range direction. For other areas coloured orange, the building block azimuth is falling into the range of 15-45 deg. The dark green coloured areas are covered by vegetation, and the blue ones denote flat grounds and water.

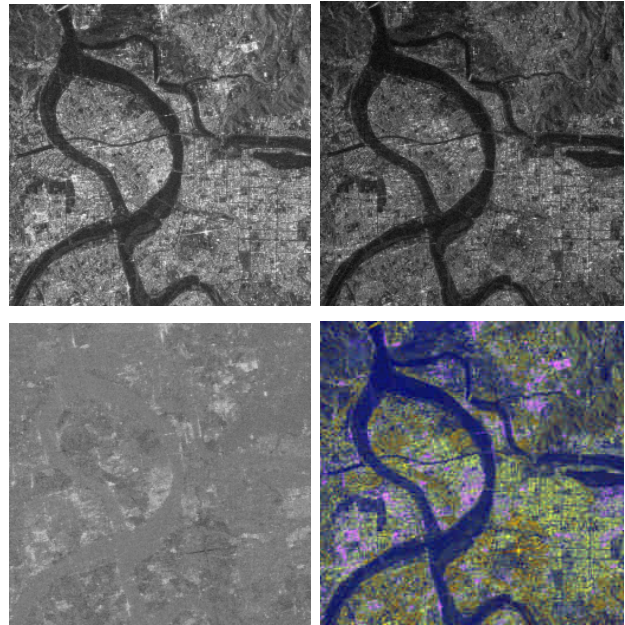


Figure 4a. A colour-coded image map (bottom-right) of the building block pattern of Taipei derived from PALSAR image pair with dual polarization: the maximal intensity (top-left); the minimal intensity (top-right); the difference image (bottom-left).



Figure 4b. The colour-coded image map of the building block patterns of Taipei as in fig. 4a is enlarged.

4. DISCUSSION

Open space (parks and water) shows the lowest intensity among other image features. People demand open space for a better urban living, and the dark (green or blue) features, corresponding to vegetation, parks and water as shown in Fig. 4b, could also be employed as one of the key factors for preparation of town planning and urban renewal projects. It has been shown that co-polarized images demonstrate the most prominent part of the intensity of radar signal, which are also sensitive to the effects of layover, dihedral reflection and Bragg scattering in the direction normal to the sensor track. Most of Taiwanese privately-owned houses, apartments and buildings under 5 stories were constructed using concrete with roof covered by metal surface, which makes strong backscattering possible. For the built-up areas, the highest intensity is observed where the building blocks are aligned with the SAR range direction. Since the azimuth of building blocks are related to the highest level of intensity, careful use has to be made of the HH-polarized images.

On the other hand, the cross-polarized images are less sensitive to the above-mentioned effects, but the intensity levels are generally much lower than the co-polarized counterparts. In some cases, the ambiguities between vegetation and built-up areas may arise in interpretation and segmentation by using single cross-polarized images alone. Using images with dual polarization can increase the chance of successful interpretation and segmentation of urban targets. It has been shown that integration of co-polarized and cross-polarized images can help to determine some interesting features of urban areas, such as a pattern map of building blocks. However, further study for applications of images with dual polarization in the context of urban environments is still required in the future.

4. CONCLUSIONS

Using SAR data with single polarization for interpretation and segmentation can result as misleading results. It is found that using SAR images with dual polarization can increase the chance of success in interpretation and segmentation. A computer-aided interpretation tool has been developed and proved to be useful for human interpreter in using SAR images with dual polarization, such as ALOS PALSAR data. Human beings are still the most effective operators, in terms of interpretation for SAR intensity images. In order to create an effective agent for SAR image interpretation, it will be useful to study more about what kind of information a human operator can extract from SAR images with multiple polarization. Then, automatic approaches for extraction of information from SAR images can be fully developed.

Acknowledgement

The ALOS PALSAR data used in this paper is provided by JAXA under Project No. PI-061. The result presented in

this paper is part of the work in project, NSC 96-2625-Z-424-001, sponsored by the National Science Council, Taiwan. Collaboration work and mutual visits between the authors are possible due to the joint project co-sponsored by the Royal Society, London, and NSC, Taiwan (NSC93-2911-I-014-001 and NSC94-2911-I-014-001).

References

- [1] Chen, P.-H. and Dowman, I., 2001. A weighted least squares solution for space intersection of spaceborne stereo SAR data. *IEEE Trans. on Geo-Science and Remote Sensing*, GE-39(2), pp. 233-240.
- [2] Chen, P.-H. and Dowman, I. J., 1996, Space intersection from ERS-1 synthetic aperture radar images. *Photogrammetric Record*, 15 (88):561-573.
- [3] Oliver, C. and Quegan, S., 1990. *Understanding Synthetic Aperture Radar Images*. Artech House Inc., Norwood, U.S.A. 479 pages.
- [4] Dowman, I.J. and Morris, A.H., 1982. The use of synthetic aperture radar for mapping. *Photogrammetric Record*, 10 (60):687-696.
- [5] Elachi C. and van Zyl, J., 2006. *Introduction to the Physics and Techniques of Remote Sensing*. 2nd ed. John Wiley & Sons Inc., New Jersey, USA. 552 pages.
- [6] Lee, J.-S., Grunes, M.R., Pottier, E. and Ferro-Famil, L., 2004. Unsupervised terrain classification preserving polarimetric scattering characteristics. *IEEE Trans. on Geo-Science and Remote Sensing*, GE-42(4), pp. 722-731.
- [7] Henderson F.M. and Xia, Z.-G., 1997. SAR applications in human settlement detection, population estimation and urban land use pattern analysis: a status report. *IEEE Trans. on Geo-Science and Remote Sensing*, GE-35(1), pp. 79-85.
- [8] Tatem, A.J., Noor, A.M. and Hay, A.I., 2004. Defining approaches to settlement mapping for public health management in Kenya using medium spatial resolution satellite imagery. *Remote Sensing of Environment*. 93(2004):42-52.
- [9] Dell'Acqua, F. and Gamba, P., 2006. Discriminating urban environments using multiscale texture and multiple SAR images. *International Journal of Remote Sensing*. 27(18):3797-3812.
- [10] Norton, 2001. *Human Geography*. 4th ed. Oxford University Press. 436 pages.
- [11] Garvin, A., 1996. *The American City: What Works, What Doesn't*. McGraw-Hill Companies, Inc. 475 pages.